Dynamic integral imaging display with electrically moving array lenslet technique using liquid crystal lens

Tai-Hsiang Jen,[1] Xin Shen,[2] Gang Yao,[2] Yi-Pai Huang,[1] Han-Ping D. Shieh,[1] and Bahram Javidi[2,*]

[1]*Department of Photonics & Institute of Electro-Optical Engineering, National Chiao Tung University, Hsinchu300, Taiwan*

[2]*Department of Electrical and Computer Engineering, University of Connecticut, Storrs, Connecticut 06269, USA*

[*]*bahram@engr.uconn.edu*

Abstract: Integral imaging (InIm) has been widely investigated for three-dimensional (3-D) display applications. Aliasing due to the lenslet arrays is one of the limitations of InIm displays. In this paper, we propose a dynamic InIm display using electrically movable liquid crystal (LC) lens array to implement the moving array lenslet technique (MALT) and to eliminate the multifacet phenomenon in the 3-D images. The improvement of the viewing quality of dynamic InIm display is experimentally verified.

OCIS codes: (110.2760) Gradient-index lenses; (110.4190) Multiple imaging; (120.2040) Displays; (230.3720) Liquid-crystal devices.

References and links

1. G. Lippmann, “Épreuvesréversiblesdonnant la sensation du relief,” J. Phys. Theor. Appl. **7**(1), 821–825 (1908).
2. H. E. Ives, “Optical properties of a lippmann lenticuled sheet,” J. Opt. Soc. Am. **21**(3), 171–176 (1931).
3. C. B. Burckhardt, “Optimum parameters and resolution limitation of integral photography,” J. Opt. Soc. Am. **58**(1), 71–74 (1968).
4. A. Stern and B. Javidi, “3D image sensing, visualization, and processing using integral imaging,” Proc. IEEE **94**(3), 591–607 (2006).
5. R. Martinez-Cuenca, G. Saavedra, M. Martinez-Corral, and B. Javidi, “Progress in 3-D multiperspective display by integral imaging,” Proc. IEEE **97**(6), 1067–1077 (2009).
6. M. Cho, M. Daneshpanah, I. Moon, and B. Javidi, “Three-dimensional optical sensing and visualization using integral imaging,” Proc. IEEE **99**(4), 556–575 (2011).
7. J. Y. Son, W. H. Son, S. K. Kim, K. H. Lee, and B. Javidi, “Three-dimensional imaging for creating real-world-likeenvironments,” Proc. IEEE **101**(1), 190–205 (2013).
8. X. Xiao, B. Javidi, M. Martinez-Corral, and A. Stern, “Advances in three-dimensional integral imaging: sensing, display, and applications [Invited],” Appl. Opt. **52**(4), 546–560 (2013).
9. J.-H. Park, J. Kim, Y. Kim, and B. Lee, “Resolution-enhanced three-dimension / two-dimension convertible display based on integral imaging,” Opt. Express **13**(6), 1875–1884 (2005).
10. C. W. Chen, M. Cho, Y. P. Huang, and B. Javidi, “Improved viewing zones for projection type integral imaging 3D display using adaptive liquid crystal prism array,” J. Display Techonol. **10**(3), 198–203 (2014).
11. X. Shen, Y. J. Wang, H. S. Chen, X. Xiao, Y. H. Lin, and B. Javidi, “Extended depth-of-focus 3D micro integral imaging display using a bifocal liquid crystal lens,” Opt. Lett. **40**(4), 538–541 (2015).
12. H. K. Hong, S. M. Jung, B. J. Lee, and H. H. Shin, “Electric-field-driven LC lens for 3D/2D autostereoscopic display,” J. Soc. Inf. Disp. **17**(5), 399–406 (2009).
13. Y. P. Huang, L. Y. Liao, and C. W. Chen, “2-D/3-D switchable autostereoscopic display with multi-electrically driven liquid-crystal (MeD-LC) lenses,” J. Soc. Inf. Disp. **18**(9), 642–646 (2010).
14. C. W. Chen, Y. P. Huang, and P. C. Chen, “Dual direction overdriving method for accelerating 2D/3D switching time of liquid crystal lens on auto-stereoscopic display,” J. Display Technol. **8**(10), 559–561 (2012).
15. Y. P. Huang, C. W. Chen, and Y. C. Huang, “Superzone Fresnel liquid crystal lens for temporal scanning auto-stereoscopic display,” J. Display Techonol. **8**(11), 650–655 (2012).
16. J. S. Jang and B. Javidi, “Improved viewing resolution of three-dimensional integral imaging by use of nonstationary micro-optics,” Opt. Lett. **27**(5), 324–326 (2002).
17. J. S. Jang and B. Javidi, “Three-dimensional integral imaging with electronically synthesized lenslet arrays,” Opt. Lett. **27**(20), 1767–1769 (2002).

#240194 Received 1 May 2015; revised 19 Jun 2015; accepted 26 Jun 2015; published 7 Jul 2015

18. S. H. Hong and B. Javidi, "Improved resolution 3D object reconstruction using computational integral imaging with time multiplexing," Opt. Express **12**(19), 4579–4588 (2004).
19. M. Martínez-Corral, B. Javidi, R. Martínez-Cuenca, and G. Saavedra, "Multifacet structure of observed reconstructed integral images," J. Opt. Soc. Am. A **22**(4), 597–603 (2005).
20. J. S. Jang, F. Jin, and B. Javidi, "Three-dimensional integral imaging with large depth of focus by use of real and virtual image fields," Opt. Lett. **28**(16), 1421–1423 (2003).
21. J. S. Jang and B. Javidi, "Improvement of viewing angle in integral imaging by use of moving lenslet arrays with low fill factor," Appl. Opt. **42**(11), 1996–2002 (2003).
22. S. T. Wu and D. K. Yang, *Reflective Liquid Crystal Displays* (John Wiley & Sons, 2001).
23. K. M. Chen, S. Gauza, H. Xianyu, and S. T. Wu, "Submillisecond gray-level response time of polymer-stablized blue-phase liquid crystal," J. Display Technol. **6**(2), 49–51 (2010).
24. S. Gauza, H. Wang, C. H. Wen, S. T. Wu, A. J. Seed, and R. Dabrowski, "High birefringence isothiocyanatotolane liquid crystals," Jpn. J. Appl. Phys. **42**(6), 3463–3466 (2003).

1. Introduction

Integral imaging (InIm) technologies have been widely investigated for three-dimensional (3-D) sensing, visualization and information processing [1–7]. InIm systems use a lenslet array or camera array to capture the direction and intensity information of the light rays from a 3-D scene and then regenerate the light rays optically to produce realistic 3-D images [5, 8]. Based on the reversibility principle, the display stage is the inverse process of the capture stage. There are some interesting works applying different display devices to improve the performance of InIm systems, such as using the polymer-dispersed liquid crystal (PDLC) with the additional lens array to obtain 3-D/2-D convertible ability and enhance the resolution [9], using the LC prism array to increase the viewing zone [10], and increasing the depth of focus by using the bifocal LC lens [11]. At the same time, the LC lens array has been used for 3-D/2-D switchable displays [12–14], and increasing the resolution by using a temporal scanning LC lens [15]. In this paper, we propose an electrically movable LC lens array to realize an InIm display. The LC lens array substitutes the polymer lenslet array, which is widely used for InIm systems. The LC lens array has the advantage of providing sub-pitch movements of the lenslet along a horizontal, vertical, or diagonal direction with different driving conditions. Such characteristic has not been achieved by conventional LC lens arrays, and it can be used for the moving array lenslet technique (MALT) in the 3-D InIm system [16–18]. The MALT can enhance the viewing quality and eliminate the effects of the multifacet structure [5, 8, 19] of 3-D images. The conventional MALT is operated by moving the lenslet array mechanically. By using the proposed LC lens array, we can realize the MALT electrically without the bulky mechanical moving device, and make a compact InIm display. This LC lens array can be combined with the widely used liquid crystal display (LCD) for glassless 3-D displays, which can be applied to many areas, such as 3-D TVs, smartphones, etc.

2. Integral imaging with moving array lenslet technique

In InIm, aliasing due to the lenslet arrays will cause the multifacet phenomenon. This phenomenon degrades the viewing quality of the reconstructed 3-D images [5, 16–19]. In the pickup stage, the light reflected from the 3-D object is recorded and sampled by an image sensor with the lenslet array. The captured images are called the elemental images (EIs). According to the Whittaker-Shannon sampling theorem, the Nyquist frequency, in cycles per radian, is [16]:

$$f_{nyq} = \frac{L}{2p}, \tag{1}$$

where p is the pitch of the lenslet, and L is the distance between the observer and the lenslet array. The under sampling due to the lenslet array will cause the multifacet structure in the reconstructed 3-D image and thus reduce the viewing quality. At the same time, the observers will see different portions of the reconstructed 3-D image through different lenslets, as illustrated in Fig. 1(a). The field of view (FOV) for the observers is composed by a series of the elemental field of views (EFOVS), which may overlap causing the reconstructed 3-D images to be divided into multiple facets [5, 19].

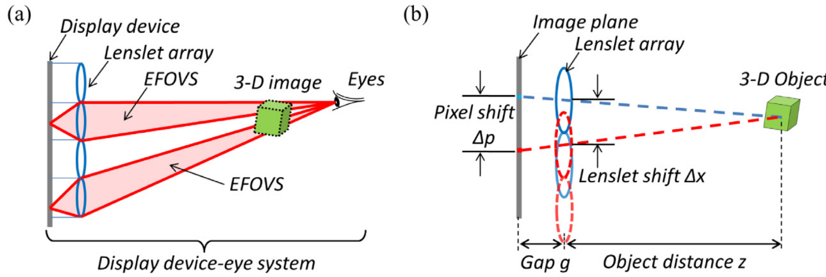

Fig. 1. (a) The illustration of the multifacet phenomenon of InIm system [19]. EFOVS are the elemental field of views. (b) The principle of the moving array lenslet technique [16].

To eliminate the multifacet effect and enhance the viewing quality, the moving array lenslet technique has been applied to an InIm display by moving the lenslet array mechanically or electrically [16–18]. In the pickup stage, the lenslet array is moved with a sub-pitch distance in a plane perpendicular to the optical axis and captures a set of EIs. The relation between the pixel shift of EIs and the shift of the lenslet array is illustrated in Fig. 1(b). The pixel shift Δp is

$$\Delta x = \frac{\Delta p}{g+z} \cdot z \approx \Delta p, \tag{2}$$

where Δx is the shifting distance of the lenslet array, g is the distance from the lenslet array to the image plane, and z is the distance from the object to the lenslet array. In the display stage, the lenslet array should move with an appropriate speed and synchronize with the corresponding EIs. The series of EIs are optically reconstructed within the visual persistence time of human eyes, thus the multifacet structure will be eliminated because the reconstructed 3-D images will be integrated in the observer's brain.

3. Electrically movable liquid crystal lens array

The electrically movable LC lens array can realize the sub-pitch movements along a vertical, horizontal, or diagonal direction without any mechanical movement for MALT. The components of an electrically movable LC lens array consists of two lenticular LC lens arrays, a half-wave film, and two linear polarizers, as illustrated in Fig. 2(a). The lenticular LC lens arrays are polarization-dependent devices, and it has a maximum focusing power when the polarization of the incident light is parallel to the LC rubbing direction. Therefore, we attached the linear polarizers on the lenticular LC lens arrays to make their transmittance axes parallel to the LC rubbing directions, and the half-wave film that is placed between two lenticular LC lens arrays is to rotate the polarization by 90°. The principle of the optical system consisting of two lenticular LC lens arrays is presented in Fig. 2(b). To make the two separated lenticular LC lens arrays focus the light at the same position on the optical axis as a lenslet array, we designed the focal lengths of the two lenticular LC lens arrays to be 7.4 mm (front) and 6.2 mm (rear), and the corresponding driving voltages are 2.8 V_{rms} (front) and 3.0 V_{rms} (rear).

#240194 Received 1 May 2015; revised 19 Jun 2015; accepted 26 Jun 2015; published 7 Jul 2015

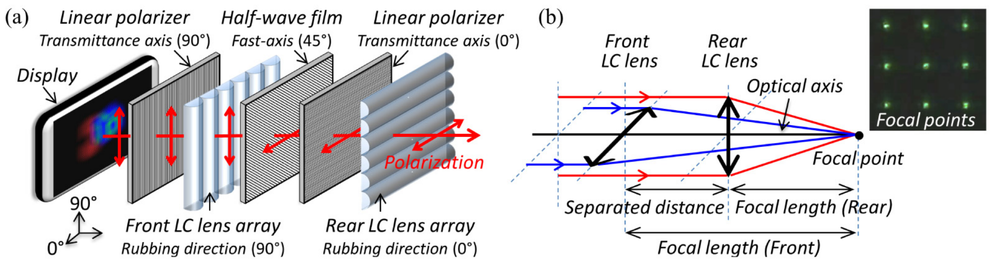

Fig. 2. (a) The components, and(b)the optical system diagram of the electrically movable LC lens array. The focal points pattern of the LC lens array is illustrated.

The multi-electrode structure of a lenticular LC lens array consists of an LC layer, a striped electrode array, a common electrode, and glass substrates, as illustrated in Fig. 3(a). The birefringence of the LC mixture (E7) is 0.216, and the cell gap is 190 µm. Previous reports suggested the optimal lenslet size for InIm as 1 mm or 2 mm [3]. Thus, we designed the LC lens array with 1 mm lens pitch. The electrode width (W_E) and electrode gap (W_S) are 50 µm, and the minimum moving step is 0.1 mm. The driving voltage is applied on the grouped electrodes to control the LC orientations, and then the LC lens will work as a cylindrical gradient-index lens. The lenticular LC lens array can realize the sub-pitch lenslet movements along the x-direction via moving the driving voltage to the next electrodes, as shown in Fig. 3(b).

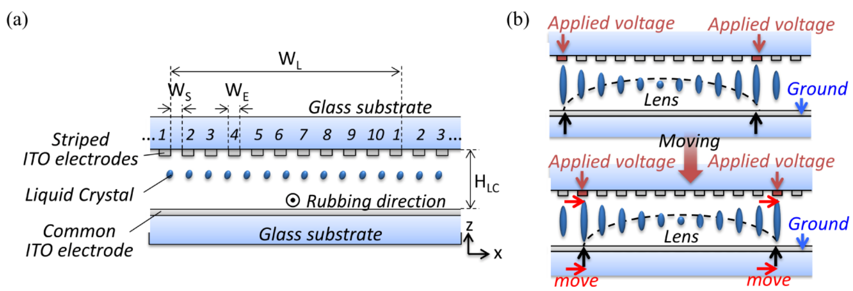

Fig. 3. (a) The electrode structure and (b) the driving method of moving lenticular LC lens array.

4. Experimental results

In the experiments, we utilized the electrically movable LC lens array to realize an InIm display. By using the electrically movable LC lens array with MALT, the viewing quality was improved, and the multifacet effect was eliminated. We performed experiments to verify the feasibility of the proposed concept. We used a smartphone (HTC ONE/M7, ~54 µm pixel size) as a display panel to display the EIs, which is controlled by a computer. The movable LC lens array was fixed on the motorized translation stage, and we adjusted the LC lens array by the electrical translation stage to accurately align to the EIs displayed by the smartphone. A Canon EOS 5DII camera with a fixed-focus lens (f = 50 mm) was placed 750 mm in front of the LC lens array to capture the 3-D images. We simulated the pickup stage using 3ds Max software and captured 96 (H) × 54 (V) EIs. The resolution of EIs is 20 (H) × 20 (V) pixels that matched with the pixel size and the resolution of the smartphone. The simulated 3-D scene is shown in Fig. 4(a). We set a letter '3′ at the distance of 60mm from the pickup pinhole camera array in the software. The distance between the center of the dice and the pinhole camera array was 20mm. In order to increase the depth range of the 3-D scene throughout the real and virtual image fields, we synthesized the EIs of the letter and the dice to be reconstructed as a virtual image and a real image, respectively [20].The letter was set to

#240194 Received 1 May 2015; revised 19 Jun 2015; accepted 26 Jun 2015; published 7 Jul 2015

be reconstructed at 60 mm behind the LC lens array, and the dice was set to be reconstructed at 20 mm in front of the LC lens array. The generated EIs are shown in Fig. 4(b).The EIs optically reconstructed the 3-D scene through the LC lens array as an InIm display. The reconstructed 3-D images from 9 different viewpoints are shown in Fig. 4(c). From different viewpoints, we can see the occlusion (or interposition) relationships between the letter and the dice. In order to make the observer unaware that the 3-D scene was reconstructed with a series of EIs by electrically moving the LC lens array, the LC lens array should be moved at least as fast as the visual persistence time (S) of the human eyes. The moving velocity (V) should satisfy [21]:

$$V = \frac{p}{S \cdot \cos\theta} \tag{3}$$

where p is the lens pitch, and θ is the angle of the moving direction. S is approximately 1/16 s, the moving velocity should be 22.6 mm/s when $\theta = 45°$ and $p = 1$ mm. In the experiments, the moving step along the diagonal direction with 45° is ~0.28 mm (0.2 mm in x- and y-directions).

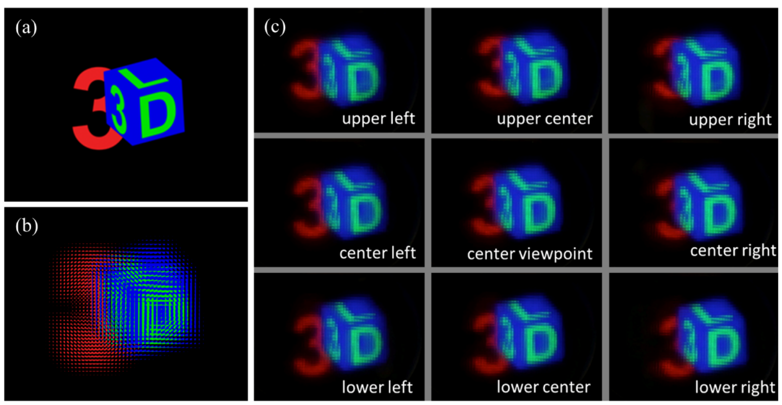

Fig. 4. (a) The simulated 3-D scene, (b) the computationally generated EIs from the 3-D scene, and (c) the reconstructed images of InIm display using the electrically movable LC lens array observed from 9 different viewpoints without MALT.

In order to satisfy the requirement of the moving velocity, each moving step of the LC lens array should be completed in 12.5 ms. However, by using the overdriving method that was used to accelerate the LC response [14], the response time of the LC lens array is ~4 s with 10 V_{rms} overdriving voltage (1 kHz, square wave). Although the current response time of the LC lens array cannot reach 12.5 ms, we can reduce the response time via reducing the cell gap and increasing the driving voltage, based on the LC response time (τ) formula as follows [22]:

$$\tau = \frac{\gamma d^2 / K\pi^2}{(V / V_{th})^2 - 1} \tag{4}$$

where γ is the viscosity, K is the elastic constant, d is the cell gap, V is the driving voltage, and V_{th} is the threshold voltage. Furthermore, the response time of the LC lens array can be further reduced via using the fast response LC material, such as blue phase LC (BP-LC) [23]. By using high birefringence LC (HB-LC) materials or Fresnel-type LC lens, the response time can be reduced because of decreasing the cell gap of the LC lens [15, 24]. By taking advantage of the novel LC materials, the response time of the LC lens array can be further improved.

#240194 Received 1 May 2015; revised 19 Jun 2015; accepted 26 Jun 2015; published 7 Jul 2015

Although the response of the electrically movable LC lens array was insufficient to satisfy the moving velocity requirement of MALT, we can utilize an indirect way to simulate the reconstructed 3-D images with MALT. In the experiment, we captured the first reconstructed image at a distance of 750 mm from the LC lens array for the result without MALT, as shown in Fig. 5(a). The F-number of the camera is set to be 16, of which the aperture diameter is ~3.1 mm, to simulate the pupil size of human eyes in an ordinary light environment [21]. Then, we electrically drove the LC lens array to sequentially move four steps along the diagonal direction (θ = 45°). For each step, we changed the corresponding EIs for the 3-D display, and captured the reconstructed image with the same camera. In the experiment, a total number of five images (one image with the original lens position and four images corresponding to the four step movements of MALT) were captured. Finally, we averaged the five captured images to obtain a time-averaged reconstructed image for the simulated result of MALT, as shown in Fig. 5(b).To compare with the image without MALT (Fig. 5(a)), the reconstructed image with MALT (Fig. 5(b)) is smooth and continuous, and the multifacet effect is eliminated. In order to evaluate the improvement of the viewing quality, we utilized two small balls with the diameters of 3 mm as a 3-D scene. The image of the 3-D scene is shown in Fig. 5(c). The green and red balls were set to be reconstructed at 20 mm and 30 mm behind the LC lens array, respectively. The experimental results show that the reconstructed image of the balls without MALT was divided by several dark lines, and the balls are square-shaped, as shown in Fig. 5(d). The intensity profile along the white line in the image had multiple peaks, as plotted in Fig. 5(f). By using MALT, the balls can be completely reconstructed, as shown in Fig. 5(e), and the intensity profile along the white line only has one peak with a smoother shape of the curve, as plotted in Fig. 5(g). Compared to the image without MALT, the objects can be recognized as two balls with circular shapes from the image reconstructed with MALT, but the objects cannot be identified from the image without using MALT. Therefore, we verified that the viewing quality of InIm display was improved by using the electrically movable LC lens array with MALT. Because of the pixelization of InIm display, the limitations on the lateral resolution and longitudinal resolutions exist. For the reconstructed 3-D images, the longitudinal resolution is lower for the distant object from the lenslet array (the red ball) compared with the closer one (the green ball).

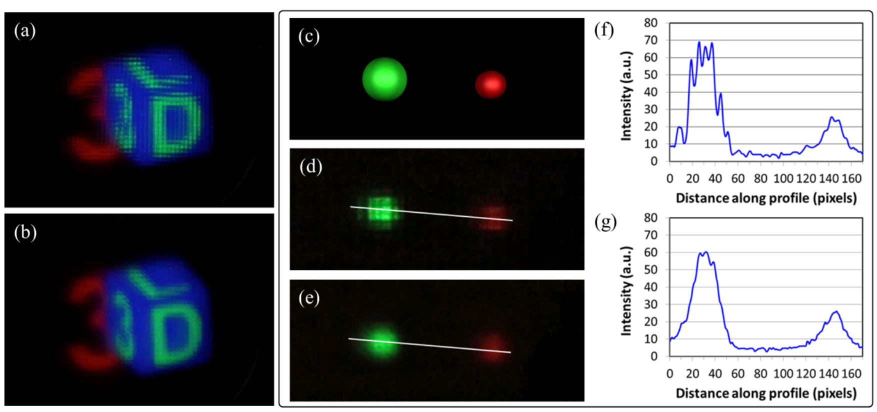

Fig. 5. The reconstructed images of the 3-D scene.(a) without MALT, and (b) with MALT.(c) Two balls with the diameters of 3 mm used as the 3-D scene; the reconstructed images of the two balls using the electrically movable LC lens array.(d) Without MALT, and (e) with MALT; (f) the intensity profile along the white line in (d), and (g) the intensity profile along the white line in (e).

#240194 Received 1 May 2015; revised 19 Jun 2015; accepted 26 Jun 2015; published 7 Jul 2015

5. Conclusion

InIm displays have been widely investigated because they can provide horizontal and vertical parallaxes and continuous varying perspectives without special viewing devices. In this paper, we have presented an InIm display by using the electrically movable LC lens array instead of the polymer lenslet array. Depending on the advantage of the two separated lenticular LC lens arrays with the multi-electrode structure, the sub-pitch movements of the lenslets along a vertical, horizontal, or diagonal direction can be realized and electrically controlled by the driving circuit. Such characteristics have not been achieved by the conventional LC lens arrays. Compared to a lenslet array that commonly used for InIm displays, the proposed LC lens array will slightly induce the cross-talk because the reflection and diffraction will happen in the separated space between two LC layers. In the experiments, the viewing quality of InIm display was increased and the multifacet effect was eliminated by using the electrically movable LC lens array with MALT. The improvement of the viewing quality of InIm display by using the proposed LC lens array is experimentally verified in an indirect way because of the long response time (~4 s) of the LC lens array. By taking advantages of new LC materials, such as BP-LC and HB-LC materials [23, 24], the response time of the LC lens can be further reduced in the future. In addition to the new LC materials, we can turn the LC lens into the Fresnel-type LC lens [15] to significantly reduce the response time for future application.

Acknowledgments

We wish to acknowledge Samsung Electronics Inc. for its support under the Samsung Advanced Institute of Technology (SAIT) Global Research Outreach (GRO) Program. The research of movable LC lens array was supported by the National Science Council in Taiwan under Grant No. NSC101-2221-E-009-120-MY3 and Innolux Corp. Additional thanks go to Jong-Guang Wei, Chia-Liang Hung, and Han-Chiang Wu at Innolux Corp. who have provided assistance.

#240194 Received 1 May 2015; revised 19 Jun 2015; accepted 26 Jun 2015; published 7 Jul 2015